Journal of Applied Polymer Science

Crystallization behavior and water vapor permeability of poly(lactic acid) nanocomposite under oscillatory shear

Zhongbin Xu,[1] Liangyao Su,[1] Shichao Jiang,[1] Wei Gu,[2] Mao Peng,[3] Pengfei Wang[1]

[1]Department of Chemical and Biological Engineering, Institute of Process Equipment, Zhejiang University, Hangzhou, 310027, China

[2]Shanghai Foreign Language School, Shanghai International Studies University, Shanghai, 200083, China

[3]Department of Polymer Sci and Engn, MOE Key Lab Macromol Synth and Functionalizat, Zhejiang University, Hangzhou, 310027, China

Correspondence to: M. Peng (E-mail: pengmao@zju.edu.cn) and P. Wang (E-mail: peng@zju.edu.cn)

ABSTRACT: The crystallization behavior and water vapor permeability of a poly(lactic acid) (PLA) nanocomposite containing 5 wt % organic montmorillonite (OMMT) under oscillatory shear were investigated. Under the oscillatory shear, OMMT platelets exhibited a better intercalated structure and oriented along the flow direction, some of the OMMT platelets are exfoliated and dispersed in the form of single or few-layer platelets. These well-dispersed OMMT platelets acted as more effective nucleating and accelerating agent for the crystallization of PLA, as a result, the cold crystallization enthalpy was significantly decreased, the cold crystallization temperature was much closer to the melting temperature and the crystallinity is dramatically increased, which are observed for the first time. Moreover, the water vapor permeability is decreased by 36% due to the barrier effect of the well-dispersed OMMT and the increased crystallinity of PLA, which increase the tortuous path that water molecules required to permeate. The mechanical properties are also enhanced owing to the well-dispersed OMMT and increased crystallinity. © 2015 Wiley Periodicals, Inc. J. Appl. Polym. Sci. **2015**, *132*, 42321.

KEYWORDS: composites; crystallization; molding; mechanical properties

Received 23 January 2015; accepted 6 April 2015
DOI: 10.1002/app.42321

INTRODUCTION

Poly(lactic acid) (PLA) is a biodegradable thermoplastic synthesized from lactic acid, which is derived from renewable resources such as corn, rice, wheat, and potatoes.[1] As the most commercially successful bio-derived polymer, PLA is widely used in biomedicine, packaging, and other short-life disposable products.[2,3] Despite the attractive biodegradability and suitability of PLA for food packaging, it exhibits poor barrier properties compared with conventional thermoplastics, with especially poor water vapor barrier property.[1–3]

Improvement in barrier properties is a notable advantage of PLA/nanoclay nanocomposites. Among the clay-based nanofillers, montmorillonite (MMT) as layered silicate has been investigated in the preparation of PLA/nanoclay nanocomposites and significant reduction in water vapor permeability has been achieved using relatively low MMT contents.[4–14]

Maiti *et al.*[5] studied the barrier properties of PLA/layered silicate nanocomposites containing smectite, MMT, and mica. The water vapor barrier property of the PLA nanocomposites was better than that of neat PLA. A larger aspect ratio of the nanoclay platelets resulted in a greater improvement in barrier property. Rhim *et al.*[6] compared the effect of three types of organic montmorillonite (OMMT), i.e., Cloisite Na+, Cloisite 30B, Cloisite 20A with different interlayer cations, on the water vapor barrier property of PLA nanocomposite. PLA nanocomposite film with 5 wt % nanoclay was prepared with a solvent casting method. A significant reduction (6–33%) in water vapor permeability was observed. Among the clays used, Choisite 20A was most effective in improving the water barrier property. Li *et al.*[7] had reported the water vapor barrier property of PLA/OMMT nanocomposites prepared by solution intercalation. The X-ray diffraction and transmission electron microscopy indicate that OMMT platelets are well intercalated and the interlayer spacing is increased. A 23.9% reduction in water vapor permeability was observed at a loading of 5 wt % OMMT. Duan *et al.*[8] investigated the water vapor permeability of PLA nanocomposites blended with MMT. PLA nanocomposites containing 1–6 wt % MMT were prepared by melt compounding and subsequent compression molding. The nanocomposite containing 5 wt % MMT exhibited an intercalated structure, and a 40% reduction in water vapor permeability was observed.

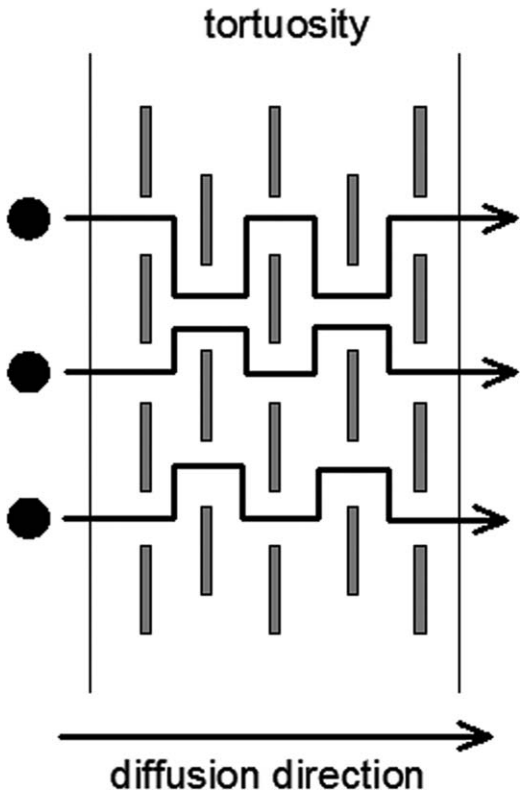

Figure 1. Schematic diagram of the tortuous path model.

Zenkiewicz *et al.*[9] studied the barrier properties of PLA/MMT nanocomposites with different blowing ratios. The PLA/MMT nanocomposite film exhibited the best barrier property when the stretch ratio was 4. Transmission electron microscopy (TEM) indicated that the shear flow of blow molding led to the formation of ribbon-structured MMT platelets in the PLA matrix, with the platelets arranged parallel to the flow direction. The ribbon-structured MMT platelets remarkably increased the tortuous path of water and gas molecules, resulting in a low permeability through the PLA/MMT nanocomposite film. Thellen *et al.*[10] employed the same blow molding process and reported improved water vapor barrier property with a 50% reduction in water vapor permeability when 5 wt % MMT was added to the PLA nanocomposite.

The improved barrier properties of such polymer nanocomposites are generally attributed to the tortuous path, in which gas or liquid molecules experience an increased diffusion path length because of the impervious clay platelets. The "tortuous path" model is schematically illustrated in Figure 1, assuming rectangular clay platelets aligned perpendicular to the diffusion direction.[15] The improvement in the water vapor property of polymer nanocomposites depends on the volume fraction of nanoclay, the aspect ratio of the platelets and their orientation.[16] On the other hand, some studies are reported that the high crystallinity is benifit to the water vapor barrier property of PLA. Shogren[17] measured the water vapor transmission rate of crystalline and amorphous PLA and reported an activation energy of 5 kJ mol^{-1} for amorphous PLA and a negative activation energy of 0.1 kJ mol^{-1} for crystalline PLA. The crystalline PLA can be considered as a restrict region that water molecule is difficult to permeate compared with amorphous PLA. Duan *et al.*[18] measured the water vapor permeabiliy through the samples of PLA of different crysatllinity. It was found that the measured value of water vapor permeability decreased linearly with increasing crystallinity of the PLA from 0% to 50%.

Oscillatory shear flow is a repetitive shear flow, with a periodical shear rate and shear stress. It causes a strong, intermittent shear flow to the melt polymer. The dispersion and morphology of nanoclays in polymer nanocomposites were reportedly different when being processed under oscillatory shear.[19–22] Dynamic packing injection molding (DPIM) has been used to apply a low-frequency (~0.3 Hz) oscillatory shear to polymers or polymer nanocomposites during injection molding.[23,24] It can induce the orientation of macromolecular chains or nanoadditives along the flow direction. Xiao *et al.*[19] investigated the dispersion and mechanical properties of polypropylene (PP)/multiwall carbon nanotube (MWNT) nanocomposites under DPIM, and both tensile strength and impact strength of the PP/MWNT nanocomposite containing 0.6 wt % MWNTs were increased. These improved mechanical properties were attributed to the uniform dispersion and orientation of nanotubes induced by the shear stress. Yang *et al.*[20] studied the shish-kebab structure of high-density polyethylene (HDPE)/MWNT nanocomposites under DPIM. A high orientation of MWNTs in HDPE matrix was achieved with carbon nanotubes as a shish structure and HDPE lamellae as kebabs in shish-kebab entities.

To the best of our knowledge, there is no report on the crystallization behavior and water vapor permeability of polymers/OMMT nanocomposites prepared by oscillatory shear, in which the OMMT platelets are orientated along the flow direction. Herein, we investigate the effect of oscillatory shear on the crystallization behavior and water vapor permeability of PLA/OMMT nanocomposite. The crystallization behavior, intercalated structure, water vapor permeability, and mechanical properties of PLA nanocomposite are investigated.

EXPERIMENTAL

Materials

PLA (ROVE101, Haizheng Co., Zhejiang, China) was used as the polymer matrix in the nanocomposite. PLA was obtained as pellets, and had a melt flow rate of 2–10 g 10 min^{-1} (190°C, 2.16 kg), melting temperature of 150°C, and destiny of 1.24 g cm^{-3}. OMMT (DK2, FengHong, Zhejiang, China) was used as received.

Preparation and Processing of the PLA Nanocomposite

Neat PLA, PLA/OMMT nanocomposite, neat PLA processed under oscillatory shear (denoted OS-PLA) and PLA/OMMT nanocomposite processed under oscillatory shear (denoted OS-PLA/OMMT) were prepared. PLA nanocomposite containing 5 wt % OMMT was prepared in an internal mixer at 185°C for 20 min. Then, four samples of thickness 1 mm were processed on a multi-pass processing device. This purpose-built device integrated the oscillatory shear action with sample molding, and is shown schematically in Figure 2.

Dried PLA or PLA/OMMT nanocomposite pellets was added into the mold, heated to 185°C, and held at the temperature for

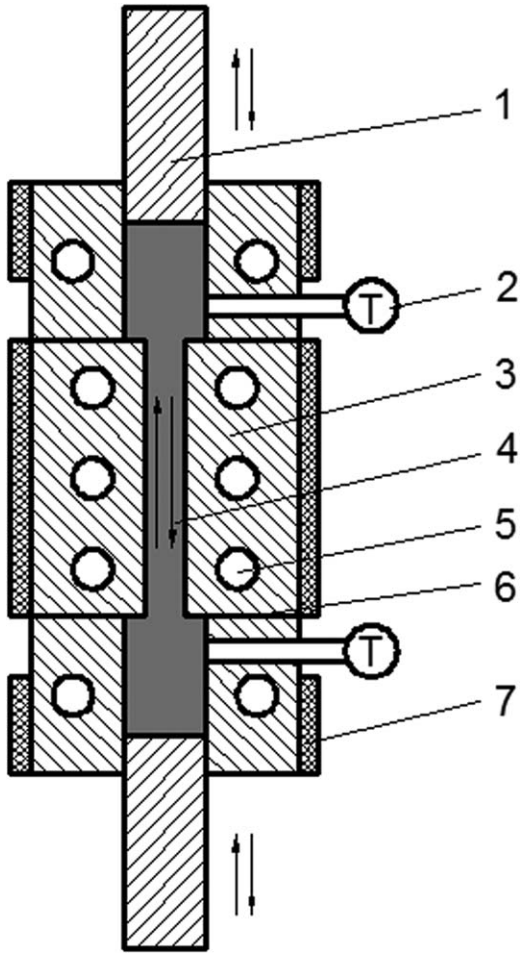

Figure 2. Schematic diagram of the multi-pass processing device. 1, piston; 2, temperature and pressure transducer; 3, mold; 4, melt; 5, water channel; 6, connector; 7, heater.

10 min. The melt was then pressed by pistons. The pressure of the mold cavity was held at 1 MPa to exclude bubbles from the melt. Plate-like neat PLA and PLA/OMMT samples were obtained during cooling process.

An oscillatory shear was applied during the processing of OS-PLA and OS-PLA/OMMT. When the pressure of the mold cavity was held at 1 MPa, the melt was moved repeatedly within the mold by two pistons moving reversibly at 0.5 Hz and with amplitude of 20 mm. The shear rate of the melt near the mold wall was about 32 s^{-1}. The pistons were stopped after 5 min and then the sample was cooled at the same rate for neat PLA and PLA/OMMT to yield OS-PLA and OS-PLA/OMMT.

Characterization

X-ray Diffraction. X-ray diffraction (XRD) was used to examine the intercalation and exfoliation structure of the OMMT platelets within the PLA matrix. XRD patterns were recorded on a Rigaku Diffractometer (Rigaku, Japan) using Cu-K_α radiation ($\lambda = 1.54$ nm) at room temperature. Diffraction patterns were recorded from 1.5 to 10° at a scanning rate of 2° min^{-1}. The interplanar spacing was calculated using the Bragg equation.

TEM. Samples of PLA nanocomposites for TEM analysis were prepared by cutting pyramid-shaped points, and then shaving off about 100-nm-thick slices at room temperature using an ultra-microtome. The sample slices were dispersed in deionized water, the suspension was added to the standard copper mesh to let it dry before being observed using a JEM-2010 microscope (JEOL, Japan) at 100 kV.

Differential Scanning Calorimetry (DSC). A DSC-7 instrument (PerkinElmer, USA) was used to investigate the melting and crystallization behavior of PLA nanocomposite samples. About 7 mg of samples were sealed in aluminum pans and heated from 30 to 190°C with a heating rate of 10°C min^{-1}. Reported values are the average of three measurements. The crystallinity (X_c) was calculated from:

$$\%X_c = \frac{\Delta H_m - \Delta H_c}{\Delta H_o} \times 100 \quad (1)$$

where ΔH_m (J g^{-1}) is the measured heat of fusion (melting enthalpy), ΔH_c (J g^{-1}) is the enthalpy of cold crystallization, and ΔH_o (J g^{-1}) is the theoretical melting enthalpy of 100% crystalline PLA (93 J g^{-1}).[25]

Water Vapor Permeability

Water vapor permeability through PLA nanocomposite sheets was measured according to standard ASTM E96-00 (2000), at 38°C and relative humidity of 90%. The water vapor permeability (P_v) was calculated from:

$$P_v = \frac{\Delta m \cdot d}{A \cdot t \cdot \Delta p} \quad (2)$$

where Δm (g) is the weight change, d (m) is the sample thickness, A (m^2) is the test area, t (s) is the time taken for Δm to occur, and Δp (Pa) is the vapor pressure difference.

Tensile Test

The tensile test was carried out on the Reger 3010 tensile testing machine (Reger, Shenzhen, China) at 23°C. A cross-head speed of 2 mm/min was used in the test. The specimens were cut along the oscillatory shear direction. In the tensile tests, five specimens were measured and the average values of the tensile strength and elongation at break were presented.

RESULTS AND DISCUSSION

Dispersion of OMMT Platelets in the PLA Matrix

The orientation and dispersion of OMMT platelets in the PLA matrix were investigated by XRD and TEM. XRD patterns of OMMT, PLA, PLA/OMMT, and OS-PLA/OMMT are shown in Figure 3. The strongest intensity peak for OMMT has a 2θ value of 3.5°, corresponding to an interlayer spacing of 2.51 nm. Compared with the pattern of OMMT, the strongest intensity peak occurs at a lower 2θ value of 2.4° in the pattern of PLA/OMMT, suggesting a better-intercalated dispersion with the interlayer spacing of OMMT platelets increasing from 2.51 to 3.68 nm. Similar results have been reported by other researchers. Duan *et al.*[8] have reported that Cloisite® 30B has an interplanar spacing of 1.84 nm, which increases to 3.4 nm in PLA

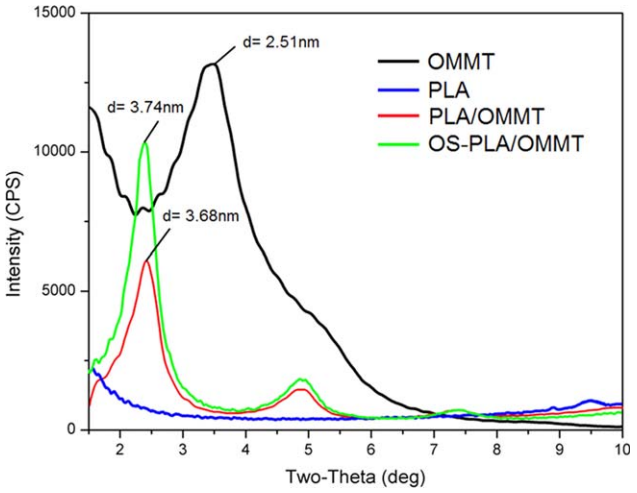

Figure 3. XRD patterns of OMMT, neat PLA, PLA/OMMT, and OS-PLA/OMMT. [Color figure can be viewed in the online issue, which is available at wileyonlinelibrary.com.]

nanocomposites produced by melt compounding. Thellen *et al.*[10] reported that the interplanar spacing of OMMT was 1.87 nm and was increased to 3.2 nm in PLA nanocomposite produced by blown film extrusion. The strongest intensity peak in the pattern of OS-PLA/OMMT appeared at the slightly lower 2θ of 2.36° than that in the pattern of PLA/OMMT. This corresponds to an interlayer spacing of 3.74 nm which demonstrates a widening of the clay interplanar spacing and a better intercalation has been achieved when the oscillatory shear was applied.

TEM observation was conducted to provide a directly understanding of the microstructure of OMMT in PLA. Figure 4 shows TEM images of PLA/OMMT and OS-PLA/OMMT at various magnifications. Figure 4(a) shows OMMT platelets randomly dispersed in the PLA matrix of PLA/OMMT. The high magnification image shows tactoid formation, intercalation, and dispersion throughout the PLA matrix. A 400k× magnification TEM image of PLA/OMMT is shown in Figure 5. OMMT aggregates with several tens of layers of clay platelets are observed. At the edge of the OMMT particles, some thin platelets can be observed, which can be ascribed to the exfoliated or partially exfoliated OMMT platelets.

Figure 4(b) shows OMMT platelets in OS-PLA/OMMT oriented in one direction, which was induced by the oscillatory shear. The high magnification image shows a significant ordering structure along the flow direction, and the uniform distribution of clay platelets throughout the whole area. A 200k× magnification TEM image of the clay platelets in OS-PLA/OMMT is

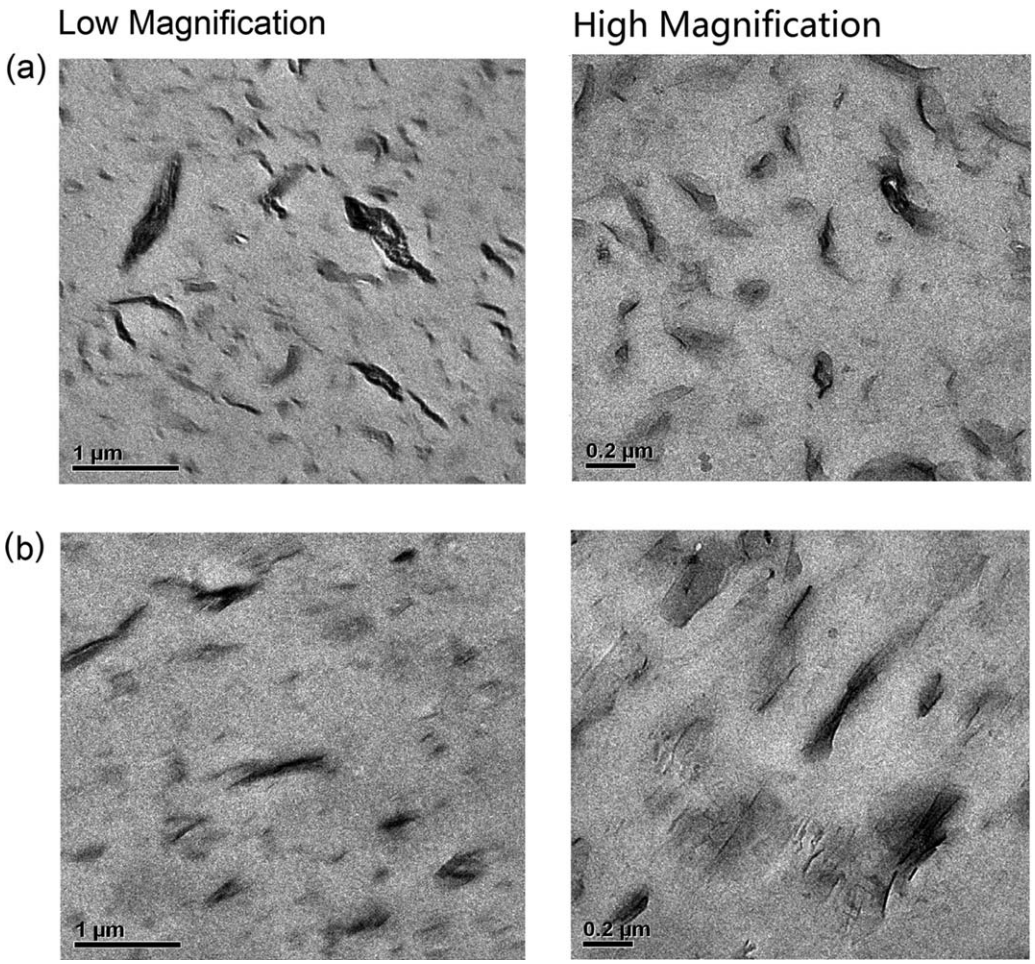

Figure 4. TEM images of (a) PLA/OMMT and (b) OS-PLA/OMMT.

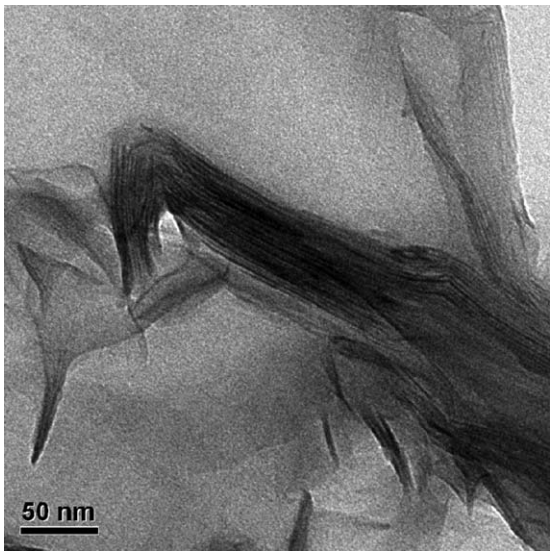

Figure 5. 400k× TEM image showing clay platelets in PLA/OMMT.

shown in Figure 6, in which intercalated OMMT aggregates are still observed, but with a thickness smaller than that in PLA/OMMT nanocomposites, suggesting that oscillatory shear reduces the size of OMMT thickness and thus increases the total area of OMMT in the matrix. Moreover, extremely thin fibrils are clearly visible, as denoted by the arrows, suggesting that part of OMMT exist in the form of single or few-layer platelets in the matrix. Such exfoliation of OMMT in PLA matrix cannot be observed in the TEM image of PLA/OMMT in Figure 5.

Crystallization Behavior

DSC curves of the first heating scan for PLA, OS-PLA, PLA/OMMT, and OS-PLA/OMMT are shown in Figure 7. The results of all samples are summarized in Table I. The presence of an endothermic peak at around 52°C was observed for the four samples, which can be ascribed to the glass transition

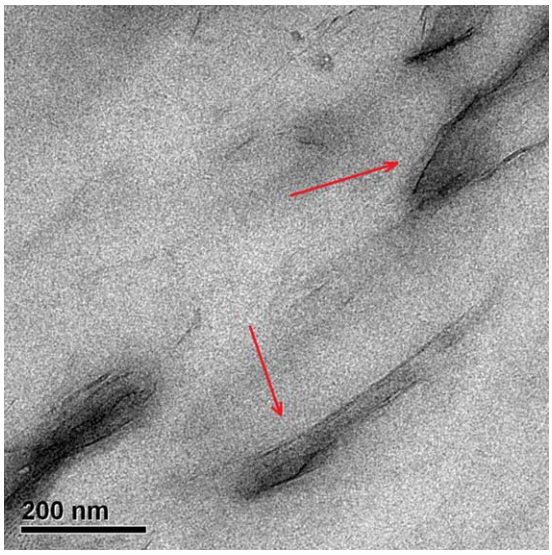

Figure 6. 200k× TEM image showing clay platelets in OS-PLA/OMMT. [Color figure can be viewed in the online issue, which is available at wileyonlinelibrary.com.]

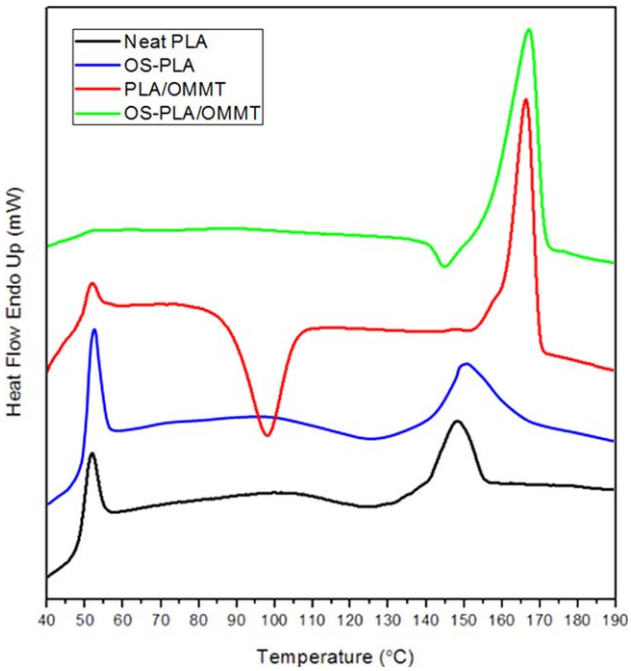

Figure 7. DSC curves of neat PLA, OS-PLA, PLA/OMMT, and OS-PLA/OMMT. [Color figure can be viewed in the online issue, which is available at wileyonlinelibrary.com.]

temperature (T_g). Addition of OMMT leads to the slightly increased T_g. Furthermore, oscillatory shear obviously reduces the endothermic peak at T_g. For OS-PLA/OMMT, the T_g peak becomes very weak and the peak value is slightly increased. The endothermic peak is owing to the structural relaxation of the polymer chains, in which the polymer chains are rearranged in a more favorable energetic configuration. The slight increase in T_g and significant decreased endothermic peak can be explained by the confinement effect of OMMT platelets which reduces the chain mobility of PLA macromolecules.

The crystallinity (X_c) and the crystallization process of PLA, OS-PLA, PLA/OMMT, and OS-PLA/OMMT were remarkably different. The DSC curve shows that the neat PLA is semicrystalline, with a very low crystallinity of 1.2% and a melting temperature of 148°C. At above the temperature of T_g, the cold crystallization process is very soft with the cold crystallization peak of 126.9°C. Compared with neat PLA, OS-PLA, processed under oscillatory shear and without addition of OMMT, showed a slightly increased crystallinity, from 1.2 to 4.0%, while the melting temperature and cold crystallization temperature were almost the same. This is mainly because that in the oscillatory shear of this study, the melt is forced to flow repeatedly in the mold cavity leading to a more uniform heat transfer in the melts and orientation of PLA macromolecules, while the cooling condition was the same in preparing the samples.

For PLA/OMMT containing 5 wt % OMMT but without processing under any oscillatory shear, a very substantial difference appeared in the DSC thermogram of the nanocomposite. An obvious exothermic crystallization peak was observed at around 98°C and the melting peak at around 166°C becomes very

Table I. DSC Data from PLA, OS-PLA, PLA/OMMT, and OS-PLA/OMMT

	T_g (°C)	T_c (°C)	H_c (J g^{-1})	T_m (°C)	H_m (J g^{-1})	X_c (%)
PLA	51.6 ± 0.3	126.9 ± 0.7	5.6 ± 0.5	148.2 ± 0.3	6.6 ± 0.4	1.2
OS-PLA	52.3 ± 0.5	124.0 ± 0.4	4.0 ± 0.7	150.5 ± 0.2	7.7 ± 0.4	4.0
PLA/OMMT	52.5 ± 0.4	98.2 ± 0.3	28.3 ± 0.2	166.2 ± 1.0	40.7 ± 0.5	13.3
OS-PLA/OMMT	52.8 ± 0.5	144.3 ± 0.1	6.7 ± 1.2	166.4 ± 0.2	40.4 ± 0.3	36.3

larger. The obvious exothermic crystallization peak is ascribed to the molecular chain reordering in the amorphous phase or cold crystallization during the heat scanning. The incorporation of OMMT platelets into PLA matrix results in the shifting of cold crystallization temperatures to lower temperatures with a very sharp exothermic peak. The decrease of the crystallization temperature and a larger enthalpy of cold crystallization may be attributed to the nucleating effect of OMMT in PLA matrix which increases the crystallization rate. At the same time, the higher melting temperature indicates that the PLA crystals in PLA/OMMT nanocomposite have less defects than that in pure PLA. The crystallinity was improved to 13.3% for PLA/OMMT. These results are in agreement with other published DSC data for PLA nanocomposite. For example, Li *et al.*[7] have reported that the DSC thermograph of PLA nanocomposites containing various OMMT platelets show a large downward exothermic peak while no such peak appeared in pure PLA, indicates that the nucleation effect induced by the OMMT platelets causes the energy release in cold crystallization process. Moreover, PLA nanocomposite containing 3 wt % OMMT obtains a highly increased crystallinity, the degree of crystallinity increased by 21.5%, 5.7 times as much as that of pure PLA. Thellen *et al.*[10] also observed that pure PLA shows a soft shoulder after the T_g in DSC thermograms and the shoulder is rendered sharper by the introduction of OMMT.

Compared with PLA/OMMT, OS-PLA/OMMT, containing a 5 wt % OMMT and processing under oscillatory shear, exhibited an enhanced crystallization process and a greatly improved crystallinity. A small enthalpy of cold crystallization was observed in OS-PLA/OMMT and the temperature of the cold crystallization peak (T_c) was at 144.3°C, which was very close to the melt temperature of 166.4°C. This phenomenon has not been reported by the other published DSC data of PLA/OMMT nanocomposite. This interesting founding indicates that PLA/OMMT nanocomposite has a faster crystallization rate and more perfect crystal structure when the oscillatory shear is applied. On the other hand, the melting enthalpy and melting temperature has no notable difference to those of the PLA/OMMT nanocomposite. A possible explanation to these phenomena is that the oscillatory shear forces the molten polymer macromolecular chains to move back and forth in the mold, which leads to a more uniform heat transfer during melting and the orientation of OMMT platelets in PLA matrix. Moreover, OMMT disperses more uniformly in PLA matrix and the exfoliated OMMT platelets, as demonstrated by the TEM and XRD, act as more effective nucleating and accelerating agents for the crystallization of PLA macromolecular chains.

Water Vapor Barrier Property

The calculated water vapor permeability of PLA, OS-PLA, PLA/OMMT, and OS-PLA/OMMT is shown in Figure 8. Compared with neat PLA, there is a limited decrease (about 4.3%) in water vapor permeability of the OS-PLA. However, a 27% reduction in water vapor permeability was achieved in PLA/OMMT. As reported by the previously studies,[5–13] this is mainly attributed to the large aspect ratio and surface area of the OMMT platelets, which increases the tortuous path that water molecules are required to permeate. Meanwhile, the increased crystallinity of PLA nanocomposite also benefits water vapor barrier property, because of the high resistance of crystalline regions to water vapor permeation, compared with free amorphous regions.[17,18]

OS-PLA/OMMT, containing 5 wt % OMMT and processing under oscillatory shear, exhibited a more significant improvement in water vapor barrier property relative to PLA/OMMT and OS-PLA. As shown in Figure 8, OS-PLA/MMT has a water vapor permeability of 1.43 × 10^{-11} g Pa^{-1} s^{-1} m^{-1} compared with 2.22 × 10^{-11} g Pa^{-1} s^{-1} m^{-1} of OS-PLA and 1.69 × 10^{-11} g Pa^{-1} s^{-1} m^{-1} of PLA/MMT. This can be ascribed to the orientation, good dispersion of OMMT and the higher crystallinity of PLA. Oriented, exfoliated and well-dispersed OMMT platelets can significantly increase the barrier property, because water molecules need to permeate a more complex path when OMMT platelets are oriented and well-dispersed in the PLA matrix under oscillatory shear. The tortuosity of the diffusion path also reportedly depends on the state of exfoliation/intercalation and the aspect ratio of the OMMT platelets in the polymer matrix. As aforementioned, under oscillatory shear, some of the OMMT platelets exfoliated and disperse in the form of single or few-layer platelets in PLA matrix, which obviously

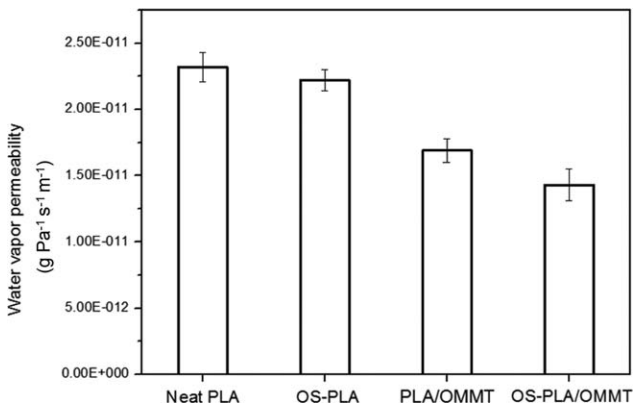

Figure 8. Water vapor permeability of neat PLA, OS-PLA, PLA/OMMT, and OS-PLA/OMMT.

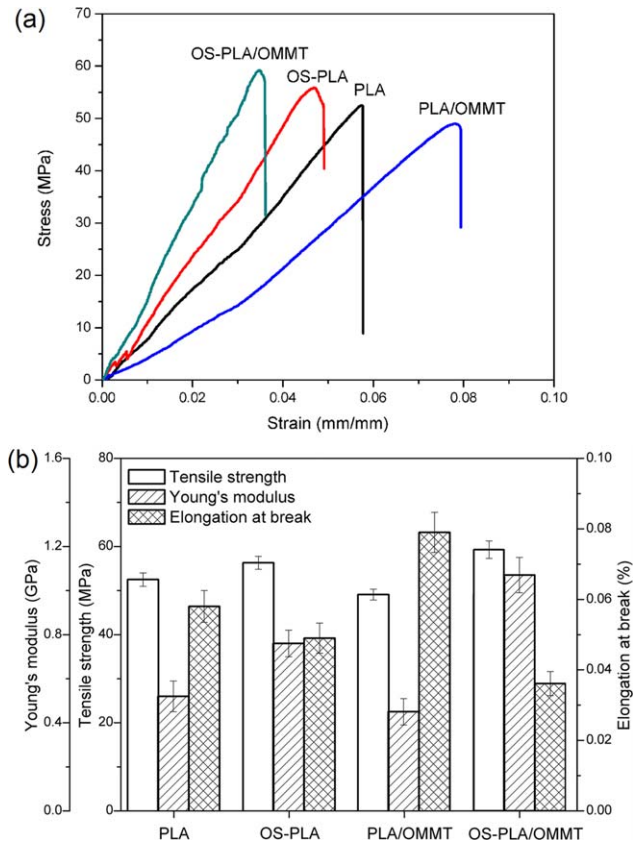

Figure 9. (a) Stress–strain curves of neat PLA, OS-PLA, PLA/OMMT, and OS-PLA/OMMT. (b) Tensile strength, Young's modulus and elongation at break of four samples. [Color figure can be viewed in the online issue, which is available at wileyonlinelibrary.com.]

increase the aspect ratio of OMMT. Furthermore, the higher crystallinity of OS-PLA/OMMT also increases the tortuous path that the water molecules are required to permeate, which improve water vapor barrier property. OS-PLA/OMMT has a higher crystallinity and the OMMT platelets are exfoliated and highly oriented, so it exhibits a better water vapor barrier property than PLA, OS-PLA and PLA/OMMT filled with randomly dispersed OMMT.

Mechanical Properties

Figure 9(a) shows the stress–strain curves of pure PLA, OS-PLA, OS-PLA/OMMT, and PLA/OMMT. The initial tensile strength, Young's modulus and elongation at break of pure PLA were 52.5 MPa, 0.52 GPa, and 5.8%, respectively, as shown in Figure 9(b). With 5 wt % of OMMT loading, the tensile strength was decreased by 6.5%, to 49.1 MPa; the Young's modulus was decreased by 13.5%, to 0.45 GPa and the elongation at break was increased by 36.2%, to 7.9%. The result is in accordance with that observed by Li *et al.*[7] In the PLA nanocomposite with the high loading (5 wt %) OMMT, many OMMT platelets formed agglomerates and tactoids, which has been directly demonstrated by TEM. The interface defects and stress concentration decrease the mechanical property. Compared with PLA, the tensile strength of OS-PLA increased by 7.2%, to 56.3 MPa; the Young's modulus increased by 46.2%, to 0.76 GPa; and the elongation at break decreased by 15.5%, to 4.9%. This is ascribed to the increased crystallinity of OS-PLA prepared under oscillatory shear. The crystalline PLA is more rigid than amorphous PLA and the crystalline region can absorb energy and stop the growth of crack in the tensile process. OS-PLA/MMT also exhibits an improved mechanical properties compared with PLA/MMT. The tensile strength was increased by 20.6%, to 59.2 MPa; Young's modulus was increased by 140%, to 1.08 GPa and the elongation at break was decreased by 45.6%, to 3.7%. The mechanism behind the enhancement of mechanical properties of OS-PLA/MMT is the better dispersion and orientation of OMMT platelets in PLA matrix when the oscillatory shear was applied. The better intercalation and exfoliated structure of OMMT platelets increase the interfacial bonding between the PLA chains and OMMT, which effectively constrains the movement of polymer chains.

CONCLUSIONS

In this study, we investigated the crystallization behavior and water vapor permeability of the PLA nanocomposite containing 5 wt % OMMT prepared under oscillatory shear. Compared with neat PLA, PLA processed under oscillatory shear receives a slightly improved crystallinity. The water vapor barrier property and mechanical properties are slightly increased. PLA nanocomposite containing a 5 wt % OMMT shows a significantly improved crystallinity from 1.2 to 13.3% and a 27% reduction in water vapor permeability. This is mainly due to the large aspect ratio and surface area of the OMMT platelets. However, the mechanical properties was decreased, this is attributes to the agglomerates and tactoids of OMMT platelets in PLA matrix when the OMMT is at high loading. When PLA/OMMT nanocomposites were prepared under oscillatory shear, the OMMT platelets are oriented along the flow direction and some of the OMMT platelets are exfoliated and disperse in the form of single or few-layer platelets in PLA matrix, which obviously increases the aspect ratio and total area of OMMT and results in the further improved crystallinity, water vapor barrier property, and mechanical properties.

ACKNOWLEDGMENTS

The work was supported by the National Nature Science Foundation of China (No. 51373153 & 51073139), the Zhejiang Provincial Natural Science Foundation of China (No. LY13E030002), and the Zhejiang Leading Team of S&T Innovation (2011R50005).

REFERENCES

1. Raquez, J. M.; Habibi, Y.; Murariu, M.; Dubois, P. *Prog. Polym. Sci.* **2013**, *38*, 1504.
2. Armentano, I.; Bitinis, N.; Fortunati, E.; Mattioli, S.; Rescignano, N.; Verdejo, R.; Lopez-Manchado, M. A.; Kenny, J. M. *Prog. Polym. Sci.* **2013**, *38*, 1720.
3. Auras, R.; Harte, B.; Selke, S. *Macromol. Biosci.* **2004**, *4*, 835.
4. Picard, E.; Espuche, E.; Fulchiron, R. *Appl. Clay. Sci.* **2011**, *53*, 58.

5. Maiti, P.; Yamada, K.; Okamoto, M.; Ueda, K.; Okamoto, K. *Chem. Mater.* **2002**, *14*, 4654.
6. Rhim, J. W.; Hong, S. I.; Ha, C. S. *LWT-Food. Sci. Technol.* **2009**, *42*, 612.
7. Li, Y.; Ren, P. G.; Zhang, Q.; Shen, T. T.; Ci, J. H.; Fang, C. Q. *J. Macroml. Sci. B.* **2013**, *52*, 1041.
8. Duan, Z.; Thomas, N. L.; Huang, W. *J. Membrane. Sci.* **2013**, *445*, 112.
9. Żenkiewicz, M.; Richert, J.; Różański, A. *Polym. Test.* **2010**, *29*, 251.
10. Thellen, C.; Orroth, C.; Froio, D.; Ziegler, D.; Lucciarini, J.; Farrell, R.; D'Souza, N. A.; Ratto, J. A. *Polymer* **2005**, *46*, 11716.
11. Tsuji, H.; Okino, R.; Daimon, H.; Fujie, K. *J. Appl. Polym. Sci.* **2006**, *99*, 2245.
12. Yourdkhani, M.; Mousavand, T.; Chapleau, N.; Hubert, P. *Compos. Sci. Technol.* **2013**, *82*, 47.
13. Tenn, N.; Follain, N.; Soulestin, J.; Crétois, R.; Bourbigot, S.; Marais, S. *J. Phys. Chem. C* **2013**, *117*, 12117.
14. Park, S. H.; Lee, H. S.; Choi, J. H.; Jeong, C. M.; Sung, M. H.; Park, H. J. *J. Appl. Polym. Sci.* **2012**, *125*, E675.
15. Nielsen, L. E. *J. Macromol. Sci. A* **1967**, *1*, 929.
16. Choudalakis, G.; Gotsis, A. D. *Eur. Polym. J.* **2009**, *45*, 967.
17. Shogren, R. *J. Environ. Polym. Degrad.* **1997**, *5*, 91.
18. Duan, Z.; Thomas, N. L. *J. Appl. Phys.* **2014**, *115*, 064903.
19. Xiao, Y.; Zhang, X.; Cao, W.; Wang, K.; Tan, H.; Zhang, Q.; Du, R. N.; Fu, Q. *J. Appl. Polym. Sci.* **2007**, *104*, 1880.
20. Yang, J.; Wang, K.; Deng, H.; Chen, F.; Fu, Q. *Polymer* **2010**, *51*, 774.
21. Wang, K.; Zhao, P.; Yang, H.; Liang, S.; Zhang, Q.; Du, R. N.; Fu, Q.; Yu, Z. Q.; Chen, E. Q. *Polymer* **2006**, *47*, 7103.
22. Yang, J.; Wang, C.; Wang, K.; Zhang, Q.; Chen, F.; Du, R. N.; Fu, Q. *Macromolecules* **2009**, *42*, 7016.
23. Gao, J.; Zhang, Q.; Wang, K.; Fu, Q.; Chen, Y.; Chen, H. Y.; Huang, H.; Rego, J. M. *Compos. Part A: Appl. S.* **2012**, *43*, 562.
24. Ning, N.; Zhang, W.; Zhao, Y.; Luo, F.; Fu, Q. *Polym. Int.* **2012**, *61*, 1634.
25. Garlotta, D. *J. Polym. Environ.* **2001**, *9*, 63.